

Upper Mantle Anisotropy Beneath Precambrian Province Boundaries, Southern Rocky Mountains

Otina C. Fox¹ and Anne F. Sheehan

University of Colorado at Boulder, Boulder Colorado

Teleseismic shear wave splitting is used to estimate mantle anisotropy beneath Precambrian province boundaries in the southern Rocky Mountains of Wyoming, Colorado, and New Mexico. Data from the passive seismic experiment of the Continental Dynamics of the Rocky Mountains (CD-ROM) project and Laramie Seismic Array are used. Data from the south CD-ROM line in New Mexico show consistent north-east fast directed shear-wave splitting, correlating with absolute plate motion and parallel to the fabric of Proterozoic accretion structures. In Wyoming, a clear change in shear-wave splitting parameters is seen across the Cheyenne Belt Archean/Proterozoic suture zone. South of the suture zone, northeast directed fast directions are observed. North of the Cheyenne Belt, shear wave splitting parameters vary with backazimuth, with the same backazimuthal patterns observed with the CD-ROM and Laramie arrays, despite the arrays being separated by over 100 km distance. This similarity in backazimuthal variation suggests a common anisotropic structure beneath both regions rather than lateral variations in anisotropy. The azimuthal variations of both the north CD-ROM and Laramie arrays are best modeled with a plunging axis of anisotropy. Our preferred model of anisotropy has an axis of symmetry that plunges steeply to the northwest. CD-ROM tomography has shown a steeply plunging fast velocity anomaly that has been forward modeled as an anisotropic slab. This feature may also be the source of the observed pattern of shear wave splitting.

INTRODUCTION

The western United States has undergone multiple deformational events that have made modifications to the original Archean and Proterozoic lithospheric structure. The Continental Dynamics of the Rocky Mountains (CD-ROM) exper-

iment was designed to explore whether one can image remnants of the ancient assembly structures preserved in the mantle or in the crust and whether these ancient structures control the style and locus of subsequent deformation [Karlstrom et al., 2002]. Archean and Proterozoic mantle may have been preserved and one can sample this ancient mantle structure through various geophysical and geochemical techniques. An alternative possibility is that the Archean and Proterozoic mantle may have been eroded away by means of more recent processes such as sub-horizontal subduction of the Farallon flat slab [Bird, 1988].

The Archean/Proterozoic suture called the Cheyenne belt in southeastern Wyoming shows zones of deformed rocks and changes in crustal structure across the suture, as inferred from

¹ Now at Alaska Earthquake Information Center, Fairbanks, Alaska.

seismic reflection and gravity studies [Johnson et al., 1984]. South of the Cheyenne Belt the general structural trend of arches and folds represents Laramide north-south deformation, while north of the suture zone there is a decrease of Laramide faulting [Ehrlich and Erlsev, 1999]. The suture zone acts as a bounding fault to deformation whose main influence could reside in the lower crust and upper mantle [Ehrlich and Erlsev, 1999]. Strike-slip movements, oblique convergence, or transpression could have caused some of the discontinuities observed across the Cheyenne Belt [Karlstrom and Houston, 1984; Duebendorfer and Houston, 1987]. We seek to explore whether these surface structural trends continue into the lower crust and mantle.

In this paper we use teleseismic shear wave splitting to determine the patterns of mantle anisotropy beneath an Archean/Proterozoic suture zone at the Cheyenne Belt in southern Wyoming and a Proterozoic/Proterozoic suture zone near the Jemez lineament in New Mexico. Mantle anisotropy can be used to infer patterns of mantle flow or the deformation history of the mantle [Tanimoto and Anderson, 1984; Schutt et al., 1998]. Previous shear-wave splitting experiments in this region have shown various results. Results from the Rocky Mountain Front experiment in Colorado mainly show null measurements (absence of shear wave splitting) with a few positive shear wave splitting measurements that do not correlate well with surface geology [Savage et al., 1996; Savage and Sheehan, 2000]. Lodore and Deep Probe experiment (western Colorado and Wyoming) shear wave splitting results have considerable spatial variability [Schutt and Humpheys, 2001], while the nearby Snake River Plain experiment produces remarkably uniform shear wave splitting results consistent with anisotropy created by absolute plate motion or the flattening of the Yellowstone plume [Schutt and Humpheys, 2001; Schutt et al., 1998]. The complexity of the Lodore and Deep Probe shear wave splitting measurements may indicate a more complex anisotropy than a single horizontal layer. In the Rio Grand Rift, the pattern of shear wave splitting has been interpreted in terms of northward-directed asthenospheric flow [Sandvol et al., 1992].

Network Descriptions

The CD-ROM passive source seismic experiment consisted of 47 broadband seismometers deployed in two north-south linear arrays (Table 1; see CDROM in back cover sleeve). The southern line (Figure 1), with 23 seismometers, crosses an inferred Mazatzal-Yavapia Proterozoic suture zone and follows the trend of the Sangre de Cristo Mountains. The northern line, consisting of 24 broadband seismometers, crosses the Cheyenne Belt, an Archean-Proterozoic suture zone near the Colorado-Wyoming border (Figure 2). The seismometers

recorded from April 1999 to June 2000. Each CD-ROM seismic station consisted of a Reftek digital data acquisition system that recorded continuously at 10 or 20 samples per second (reduced sample rate during winter months). Fifteen stations had Guralp CMG-3T seismometers; six stations used Guralp CMG-40T seismometers and 27 stations operated with Streckeisen STS-2 sensors.

The Laramie array consisted of 30 broadband seismometers (Table 2; see CDROM in back cover sleeve) at a station spacing of 1.6 kilometers, deployed from June 2000 to May 2001. The line crosses the Cheyenne Belt near Laramie, Wyoming (Figure 2). Each station in the Laramie Array consisted of Guralp 40-T seismometers recording at 1, 40 and 100 samples per second. The data were transferred by Pascal telemetry to the University of Wyoming in real time.

Shear Wave Splitting Measurements

Measurements of mantle anisotropy provide a glimpse of upper mantle structure and possible information on the past history of deformation. Mantle anisotropy is believed to be the result of lattice preferred orientation (LPO) of olivine [Nicolas and Christensen, 1987; Christensen, 1984; Ismail and Mainprice, 1998] due to finite strain. When a shear wave passes through an anisotropic region it will split into a fast and slow shear wave, with delay time between the fast and slow shear waves, δt , and will be polarized in the direction of the first arriving phase, ϕ , or fast polarization direction.

Proposed mechanisms for anisotropy in the mantle include mantle flow associated with absolute plate motion, as seen in oceanic upper mantle and certain continental areas [Tanimoto and Anderson, 1984; Vinnik et al., 1992; Schutt et al., 1998], crustal stress translating into the upper mantle [Helffrich et al. 1994], and large-scale lithospheric deformation [Russo et al., 1996; Kay et al. 1999]. The first two mechanisms reflect present day processes as the cause of anisotropy while the last would reflect "fossil" anisotropy or crust and mantle deforming coherently [Silver and Chan, 1988; Silver and Chan, 1991; Savage et al., 1990; Russo et al. 1996]. Small-scale convection has also been proposed [Sandlov et al., 1992; Savage and Sheehan, 2000]. At shallow crustal depths, other mechanisms may be present, such as alignment of cracks, presence of fluids, fractures and fissures [Crampin, S., 1994; Evans et al., 1996; Leary et al., 1990; Kuo et al., 1994; Levin and Park, 1997]. For a more complete review of anisotropy mechanisms, see the reviews by Savage [1999] and Silver [1996].

SKS waveforms were examined for earthquakes with $M_b > 5.7$ and epicentral distances $> 85^\circ$, and S waveforms were analyzed from earthquakes with depths greater than 150 km and epicentral distances of 60° – 87° (Table 3 and Table 4; see CDROM in back cover sleeve). The method of Silver and

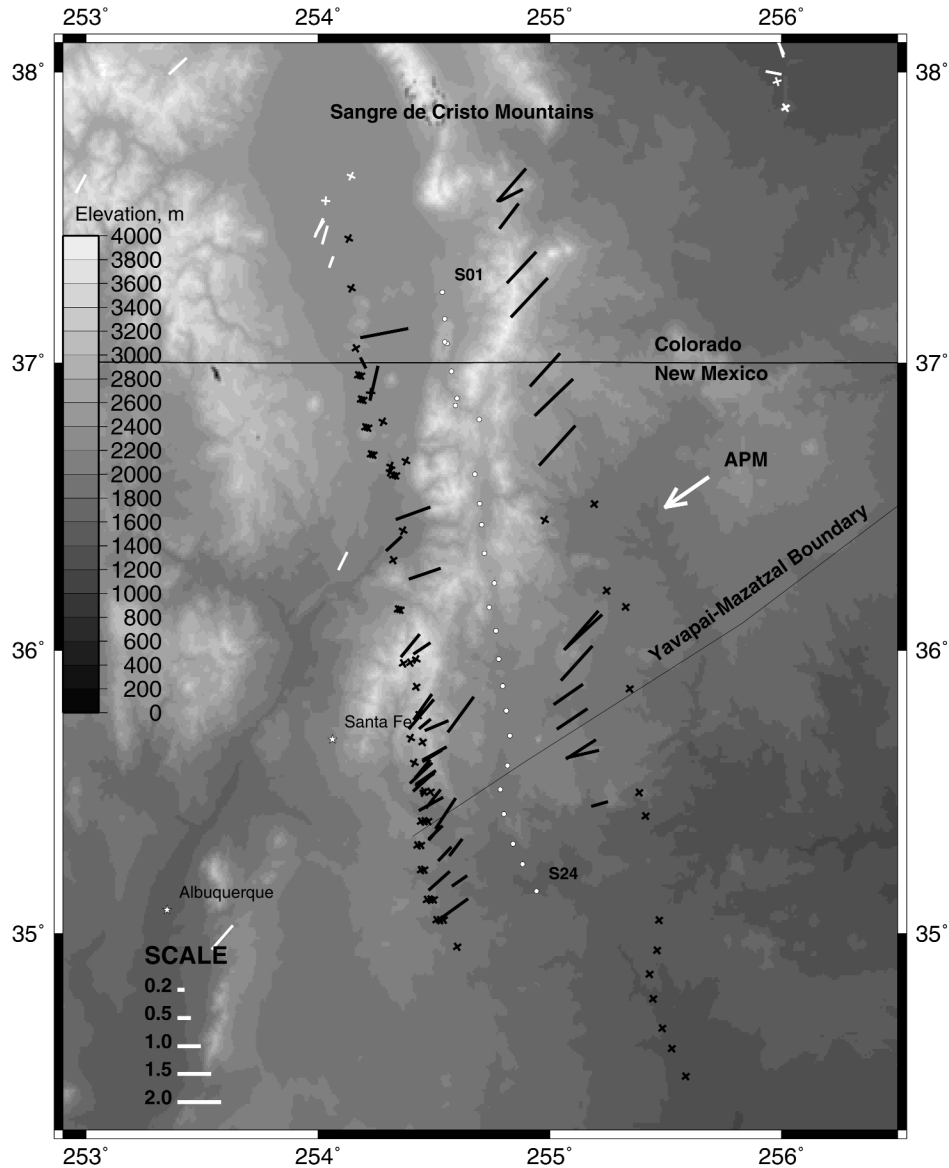


Figure 1. CD-ROM south splitting results on top of elevation map. Black lines represent splitting measurements from this study. Angle from north is ϕ and the length of the line represents δt . Black crosses represent null measurements. White lines and crosses are splitting results from past experiments. Black splits and nulls are plotted to their 220 km piercing points. S01 is in the north and S24 is in the south.

Chan [1991] is used to obtain shear wave splitting parameters. The method uses a grid search to find the values of fast polarization direction ϕ and delay time δt that best represent the splitting.

Individual splitting measurements were rated by the similarity in waveforms upon correction, the amount of reduction in tangential energy, the change from elliptical particle motion to linear particle motion, and the error plot of the grid search. Splitting measurements were rated as “great”, “good”, “ok”,

“weak” or “poor” (Table 5 and Table 6; see CDROM in back cover sleeve). In general the “weak” and “ok” splits follow the same pattern as the “good” splitting results in fast direction ϕ (Figure 3a). More scatter is seen in values of δt with the “weak” and “ok” splits (Figure 3b).

Stations with very little or no splitting are termed “null” measurements, and the incoming polarization direction is noted (dotted lines in Figure 5). Nulls are characterized by little to no tangential energy and particle motion that is not lin-

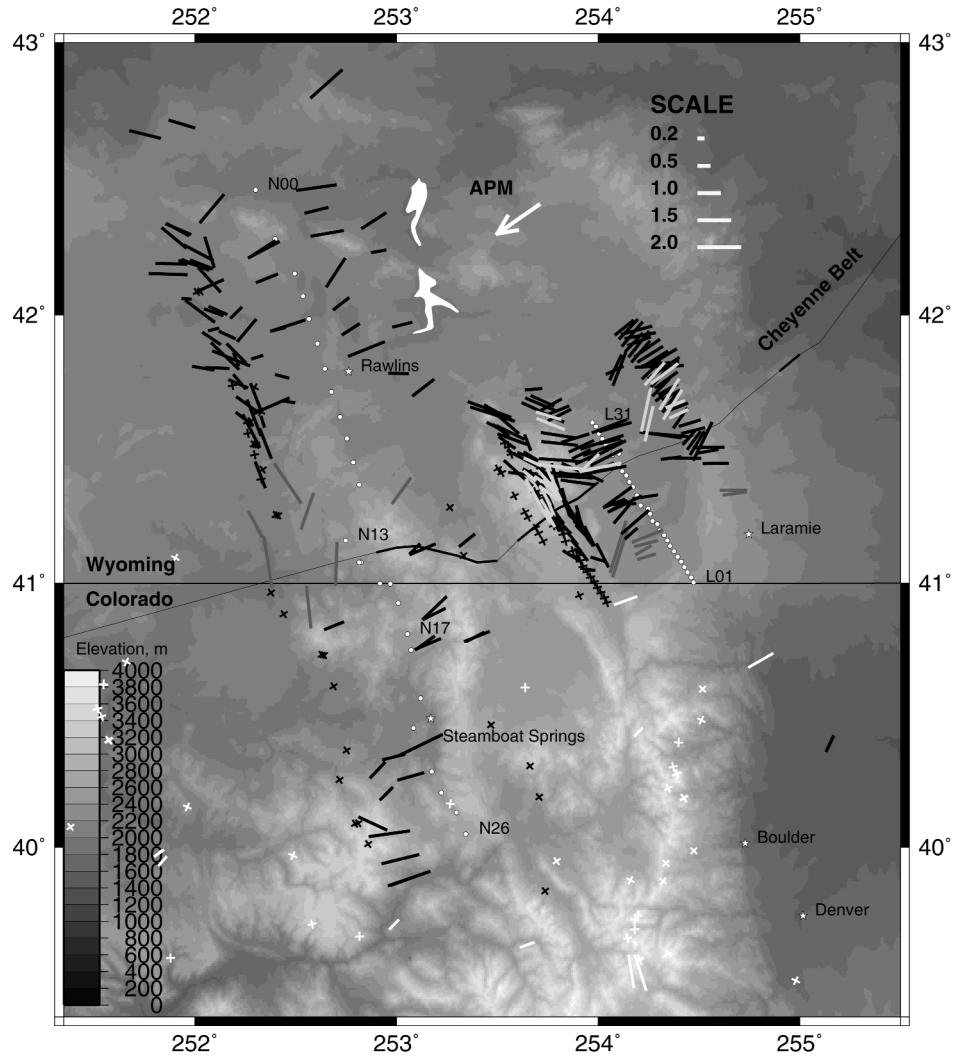


Figure 2. CD-ROM north splitting results on top of elevation map. Black and gray lines represent splitting measurements from CD-ROM and the Laramie Array. Angle from north is ϕ and the length of the line represents δt . Black crosses represent null measurements. White lines and crosses are splitting results from past experiments. Black and grey splits and nulls are plotted to their 220 km piercing points. N00 is in the north, N26 is to the south, and L01 is to the south and L31 is to the north. The Cheyenne Belt is expressed as a thick line where there is surface expression, and as a thin line where the contact is inferred. CD-ROM stations N14-N16 are medium gray. Laramie Array L01 and L02 are medium gray and stations L16, L18 and L22 are light gray.

ear. Null measurements may be due to an absence of anisotropy (isotropic conditions), vertical anisotropy with the a-axis of the olivine crystal aligned in the direction of SKS propagation, or incoming wave polarization along the fast or slow azimuth of ϕ [Savage et al, 1996]. Thus the grouping of results was in terms of positive results (great, good, ok, etc.), null results, and non-results (data neither fall under the positive or null splitting definition).

All events were uniformly filtered with a 4-pole Butterworth bandpass filter from 1–30 seconds. Thirteen events were improved (errors decreased to an acceptable range, as well as improved signal to noise ratio) by a narrower filter from 2–30s and a filter from 3–30s was used for one event. Sensitivity tests with various filters suggest that it is best to use the broadest filter possible for a noisy event. Narrower band filters may help reduce noise, but they also can increase the

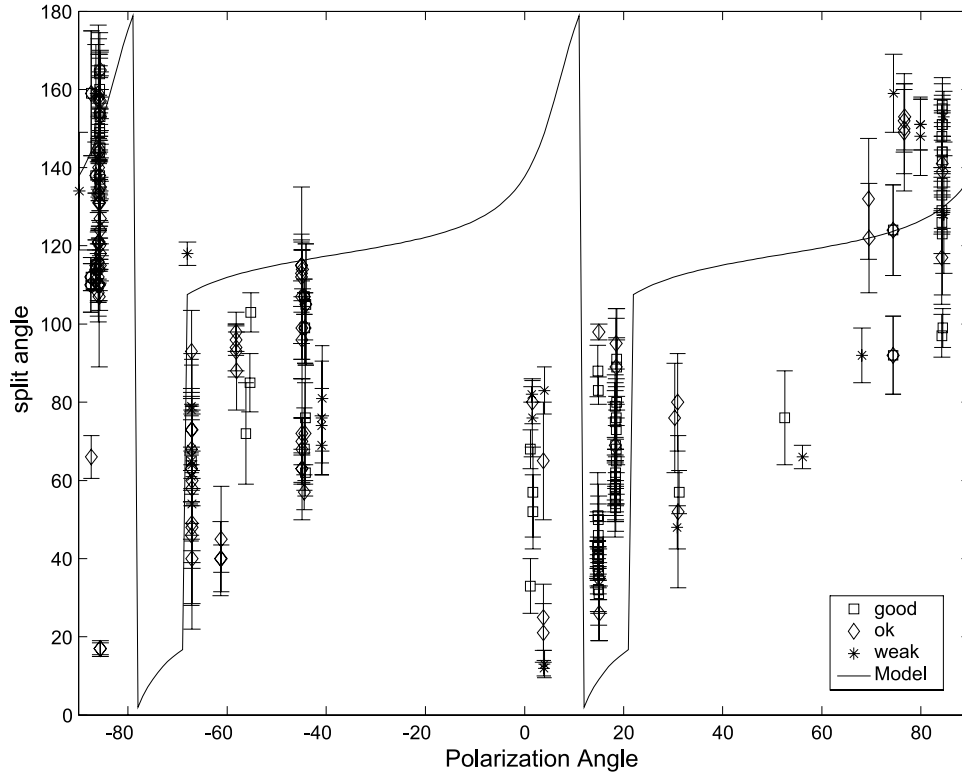


Figure 3. Two-layer model 1. $\phi_1=62^\circ$, $\phi_2=120^\circ$, $\delta t_1=0.7s$, $\delta t_2=1.5s$. Black line is 2-layer model. Dotted lines are null directions from observations. Squares represent good splitting measurements, diamonds are ok measurements and asterisks represent poor measurements. A. ϕ fit. B. δt fit.

error bars on the splitting parameters. Narrower band filters occasionally produce ok results, but the waveforms become more oscillatory.

Selection of a time window on the seismogram for analysis depends upon the noise character of the waveform as well as which window selection provides the best constrained splitting parameters. For example, windows can span the SKS, SKKS or both SKS and SKKS phases. Tests were performed using narrow, medium, and wide window length. Including both SKS and SKKS phases tends to produce more tightly constrained splitting results, in part due to the increased number of cycles that must be fit in the grid search. For a low noise event window selection can cause varying results with error bars, but little variation with ϕ and δt . In all cases the best results are achieved when the fast and slow waveforms are almost identical. With the wider windows, noise can be added into the analysis and increase the error. The narrowest windows may not include all the energy of the phase and therefore a well-constrained measurement may not be achieved. A noisy event was tested with a range of window sizes at several different stations, with variable results. On two occasions the

smaller window had the smaller error, two times the larger window had the smaller error, and once the errors were the same for both window sizes. In all cases the fast polarization directions and delay times were similar, but the size of the error bar varied with window size, in no discernable pattern.

From these examples, it can be seen that there is some analyst discretion that must be exercised to determine optimal window size. With certain stations and events there was no window that would produce an acceptable split, and therefore labeled a non-result or a poor result.

Shear Wave Splitting Results

Uniform NE-SW fast polarization directions of seismic anisotropy are with data from the CD-ROM southern line in New Mexico, while splitting from the CD-ROM northern line (Table 5; see CDROM in back cover sleeve) and the Laramie array (Table 6; see CDROM in back cover sleeve) in Wyoming show a complicated pattern that depends upon incident ray back azimuth (Figure 5; see CDROM in back cover sleeve). The shear wave splitting parameters are plotted at the pro-

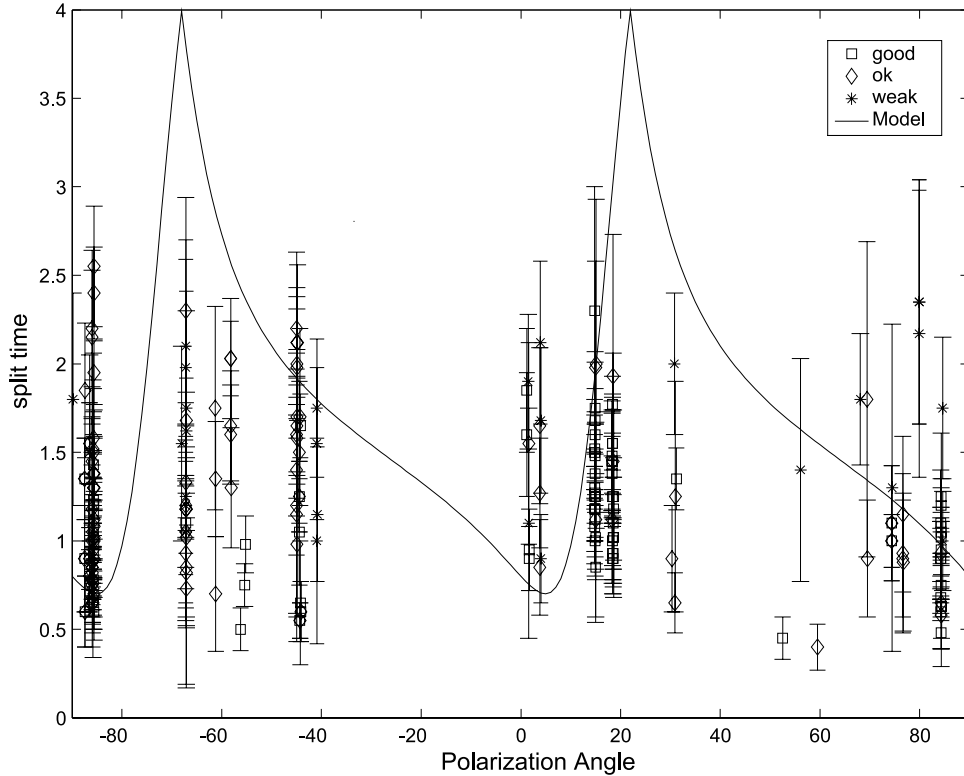


Figure 3B.

jection of their 220 km piercing points to separate back-azimuths visually (Figure 1 and Figure 2; see CDROM in back cover sleeve).

CD-ROM South Stations. The CD-ROM southern stations have a distinct 50-degree average fast polarization direction, ϕ , that correlates well with the absolute plate motion direction (Figure 1, Table 5; see CDROM in back cover sleeve). Absolute plate motion across the southern array varies between 241.7° (61.7°) in the northern part of the array to 242.4° (62.4°) in the south [DeMets et al., 1990]. Events from western back-azimuths produce shear wave splitting measurements smaller in magnitude (smaller δt) than the single good event from an eastern back-azimuth. This might suggest that the anisotropic layer is thicker to the east. Erosion from the Rio Grande Rift might be the mechanism for thinning on the western edge. Null measurements correlate well with the observed splits. Nulls from back-azimuths 236° and 237° would be coming along the fast axis and nulls from back-azimuth 141° would be arriving along the slow axis of splitting.

There is no clear shear-wave splitting evidence delineating the inferred Yavapai-Mazatzal Proterozoic-Proterozoic boundary in northern New Mexico (Figure 1). Stations throughout

the array show similar splitting parameters, and no back-azimuthal variation in ϕ is observed. The Yavapai-Mazatzal pale-accretion zone is northeasterly directed [Karlstrom and Humphreys, 1998]. Such a geometry could produce northeast directed anisotropy, thus it is uncertain whether the splitting observed is from fossil accretion or current mantle flow associated with motion of the North American plate [Vinnik et al., 1992], as both are consistent with northeast directed splitting. Splitting parameters from past experiments in the area [Sandvol et al., 1992; Savage et al., 1996] do not compare well with CD-ROM south splits in all areas, which may suggest a more complicated flow pattern or different causes of anisotropy (Figure 1). The results from the Rio Grande rift were proposed to be the result of small scale asthenospheric flow within the rift [Sandvol et al., 1992]. The extent of these northeast directed splits and consistency with APM and pale-accretion directions leads us to a different interpretation than small scale rift flow.

CD-ROM North Stations and Laramie Array. Northern CD-ROM station splitting parameters show more variation than those from the southern array, but can be separated into distinct areas (Figure 2, Figure 5, Table 5 and Table 6; see

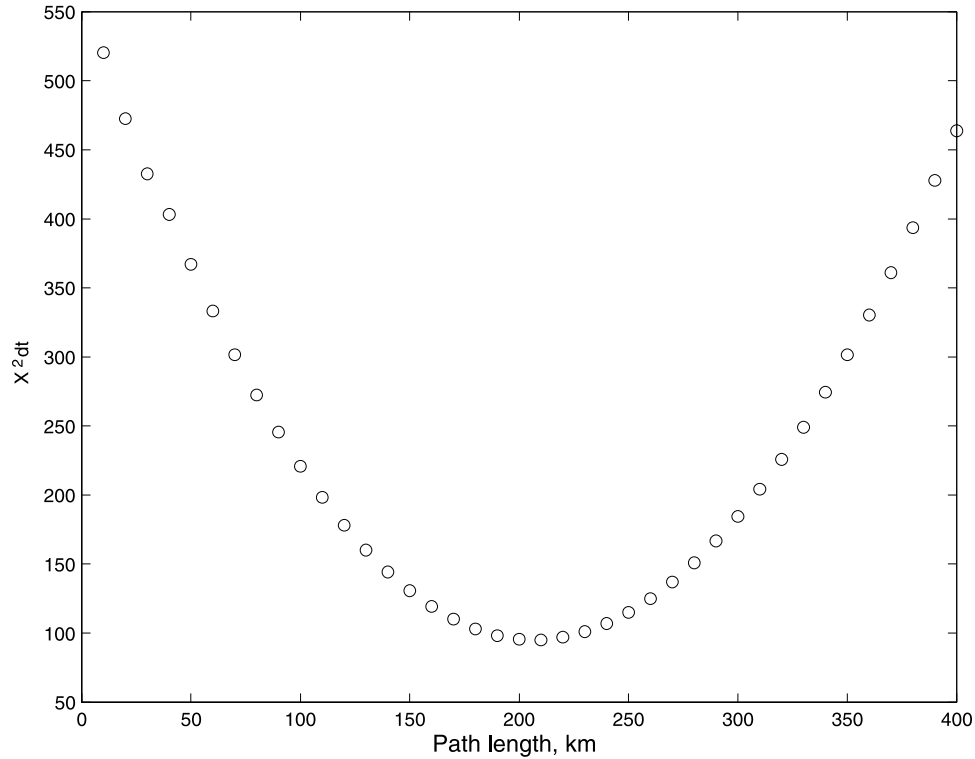


Figure 4 a. $X^2_{\delta t}$ as a function of path length for the best fitting plunging symmetry axis parameters, for CDROM stations N00 – N13.

CDROM in back cover sleeve). The southernmost stations of the north line (N17-N26), south of the Cheyenne Belt, show an average fast direction of 63° , roughly parallel with absolute plate motion direction in this region. Absolute plate motion across the northern array varies between 239.4° (59.4°) in the northern part of the array to 240.47° (60.5°) in the south part of the northern array [DeMets et al., 1990]. CD-ROM stations N14-N16 have variations different than the stations to the north or south of them (Figure 2 and Figure 4). The values of fast direction for these stations vary from 20° to -25° . These 3 stations could be imaging the anisotropic regions to the north and south, instead of being a separate anisotropic zone. CD-ROM stations N00 to N10 have a consistent back-azimuthal variation that is also observed at the Laramie array stations. At these stations events from the north to northeast and northwest back-azimuths range from 20° to 80° in fast polarization direction, while events from the west trend from 100° to 170° in fast polarization direction (Figure 4a).

The Laramie Array crosses the Cheyenne Belt north of Laramie, Wyoming (Figure 2). Variations in shear wave splitting parameters from stations within the Laramie array were examined closely to search for any variation associated with the Cheyenne Belt. The only stations with shear wave splitting

measurements with different back-azimuthal variation than the majority of the stations are the southernmost stations L01, L02 and one result from L03 (Table 6; see CDROM in back cover sleeve). When plotting the variations of CD-ROM stations N00-N13 and Laramie array stations by polarization angle, a mode-180 variation is seen with polarization angle (Figure 3). Plots of δt versus polarization angle show a wide scatter from 0.5 seconds to 2.5 seconds (Figure 3b). Models with two layers of anisotropy predict variation with a mode-90 pattern (solid black line in Figure 3) with polarization angle and back-azimuth [Ozalaybey and Savage, 1994]. This mode-90 pattern can help distinguish between a 2-layer anisotropic model and a model with a plunging symmetry axis, as the latter has a mode-360 variation with back-azimuth. These possibilities will be discussed more fully in a later section.

The backazimuthal variations in shear wave splitting polarization directions of the Laramie Array and the northern CD-ROM stations (N00-N13), are remarkably similar (Figure 4). Events from the north to northeast and northwest back-azimuths range from 20° to 80° in fast polarization direction, while events from the west trend from 100° to 170° in fast polarization direction. The consistent variation in shear-wave

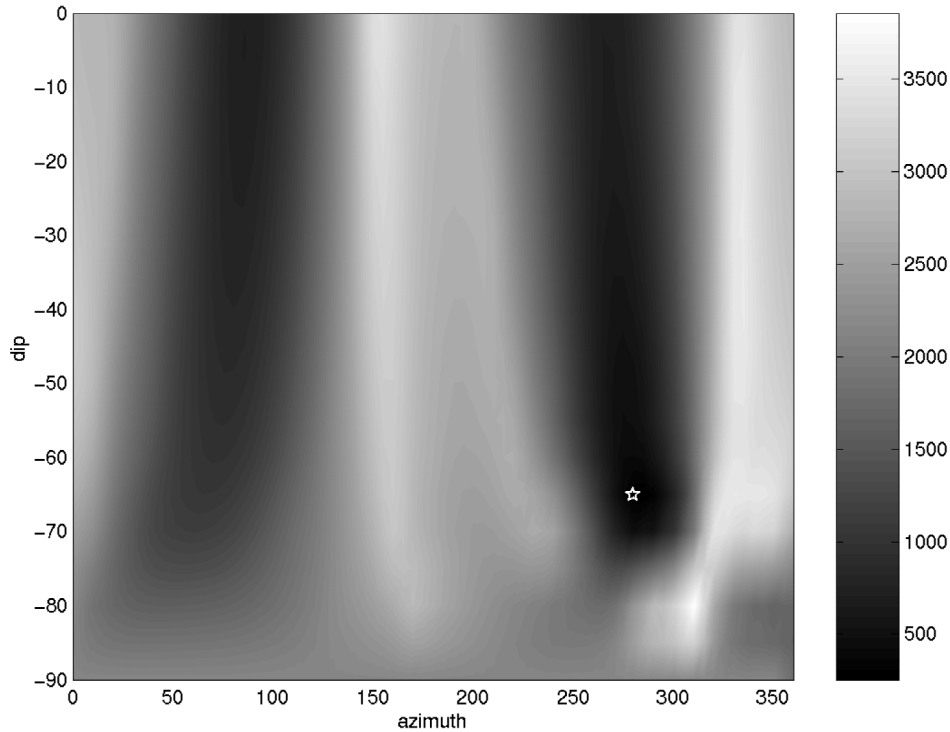


Figure 4 b. Grid search over anisotropic plunge and plunge azimuth for CD-ROM stations N00-N13. Contours represent $(X_{\delta t}^2 + X_{\phi}^2)$ for range of a-axis of orientation of olivine. White colors represent large misfit, while black represents good fit to the data. The white star is the best fitting model at plunge = 65 degrees, azimuth = 280 degrees.

splitting parameters with respect to back-azimuth between the CD-ROM and Laramie lines, despite their east-west separation by 100 km, strongly suggests a common regional mechanism for the anisotropy rather than geographically heterogeneous anisotropy.

Using fresnel zones, we can arrive at a rough depth to anisotropy estimate [Alsina and Snieder, 1995]. As stations N13 and N17 are about 40 km apart and show distinctly different shear wave splitting, it can be assumed that these two stations represent different anisotropic regions. For 8 s period waves (similar to the periods recorded in this study), Fresnel zones at 80, 200, and 440 km depth have diameters of approximately 60 km, 100 km, and 140 km, respectively. Therefore the anisotropy seen should be no deeper than 80 – 140km in depth. This would put the anisotropy in the lithosphere.

Two-layer Modeling. Two-layer modeling was performed to try and model the back azimuthal variations in shear wave splitting parameters observed at the northern CD-ROM and Laramie array stations. The forward modeling algorithm described in Ozalaybey and Savage [1994] was used in these analyses. The input parameters are the ϕ and δt for each layer.

A grid search was performed over the four splitting parameters (ϕ_1 , ϕ_2 , δt_1 and δt_2) for two layers of anisotropy, where layer 1 is the bottom layer and layer 2 is the top layer. From these grid searches, a model with a low root mean squared (rms) value was used as starting model to plot against the data to search for acceptable models. Root mean squared values are the sum of the square root of the difference of the observed and predicted values, divided by the number of values:

$$\text{rms} = \sum_i^m [(|\phi_{\text{obs}} - \phi_{\text{pred}}|^2) / n^2]^{1/2} \quad (1)$$

where ϕ_{obs} are the observed data (both ϕ and δt), ϕ_{pred} are the model predicted values (both ϕ and δt) and n is the number of input observed values.

The best fitting two-layer model is shown in Figure 3. The fast polarization for the lower layer, ϕ_1 , is 62° , parallel to absolute plate motion. The delay time, δt_1 , for the lower layer is 0.7 seconds. The upper layer has fast polarization direction, ϕ_2 , of 120° and delay time δt_2 of 1.5 seconds. This upper layer might represent some fossil lithospheric deformation. The two-layer model shown in Figure 3 is plotted versus polarization angle to show the observed data in a more detailed

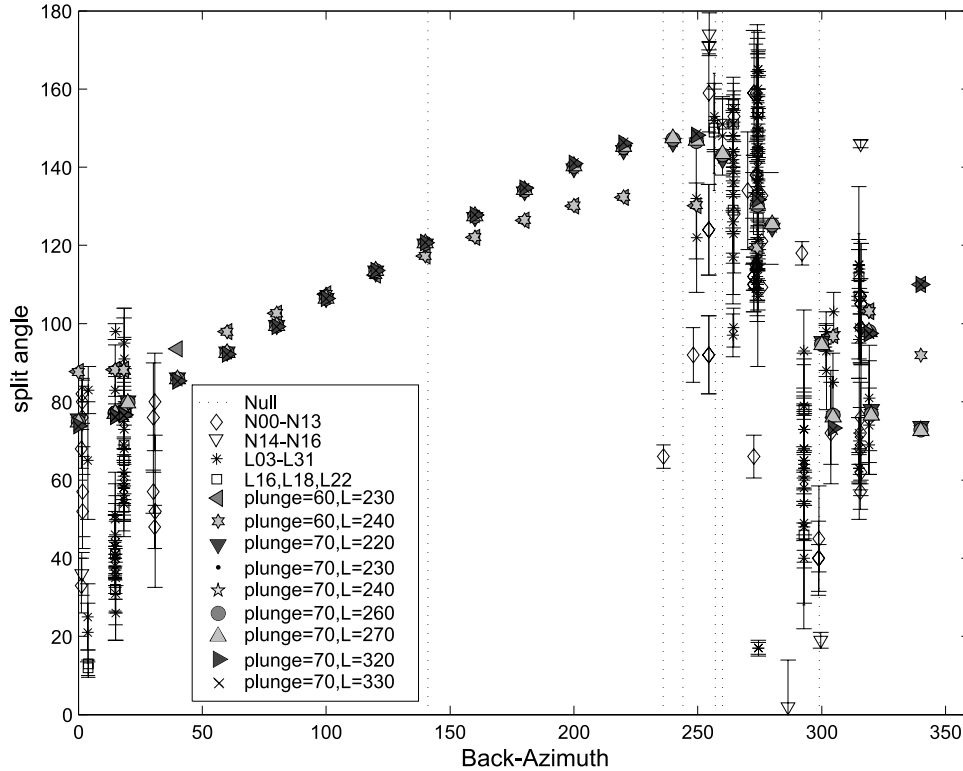


Figure 5. Models of plunging axis of symmetry. Azimuth is set at 290 degrees, plunge ranges from 60 to 70 degrees, and path length, L , varies from 220 to 330 km. Open symbols represent stations (diamonds: N00-N13, triangle: N14-N16, asterisks: L03-L31, squares: L16,L18,L22), while filled symbols are the models. Dashed lines are observed null directions. A. ϕ versus back-azimuth. Note that models for a given plunge overlap in many cases. B. δt versus back-azimuth.

way, as many back-azimuths are poorly represented. The preferred model fits the large ϕ change observed near polarization -70° (back-azimuth 280°) well as well as the ϕ -observed between polarization 70° to 90° and -90° to -95° (240° and 274° backazimuth). However the ϕ data between polarization 0° to 60° (back-azimuths 0° to 32°) are not fit well by the model. Predicted ϕ 's from this model are much larger than those observed between polarizations -70° to -40° (back-azimuths 290° to 320°). In the plot of observed δt and model δt (Figure 3b), the model does not fit the minimal variations in observed δt , nor does the model line up well with observed null measurements.

Many two-layer models fit the observed data in certain places, but none fit all the variations. There is little variation in the observed δt 's with back-azimuth or polarization angle, so it is more difficult to constrain a single model. Any anisotropic two-layer model will show 90-degree variation in both back-azimuth and polarization angle. More complete back azimuthal coverage would be needed to further distinguish between possible models. In the plot of back azimuth there is not a mode-90 variation seen clearly (Figure 4). With a mode-

90 variation there should be observed- ϕ of about 120 – 160° between polarization angles -20° to at least 5° (Figure 3). There are no observed splits between -20° to 0° polarization (Figure 3), making it difficult to constrain the model. Where there are observed shear wave splitting measurements, around polarization angle 4° , the values of observed ϕ are between 20° and 90° , which do not correlate with the observed ϕ from polarization angle -86° (110° to 165° observed ϕ).

With many models fitting the data equally well it is difficult to select a final a 2-layer model and assign meaningful uncertainties to it. One advantage of the grid search is that many poorly fitting models can be rejected, and trade-offs between parameters can be visualized. The broad class of 2 layer models that fit the data best have a lower layer of anisotropy aligned northeast to east-northeast and an upper layer of northwest to north-northwest.

Plunging Symmetry Axis Modeling. Since the stereographic projections of the data do not show 90° or 180° symmetry of splitting with backazimuth, models with a plunging symmetry axis of anisotropy are tested. Hartog and Schwartz [2000]

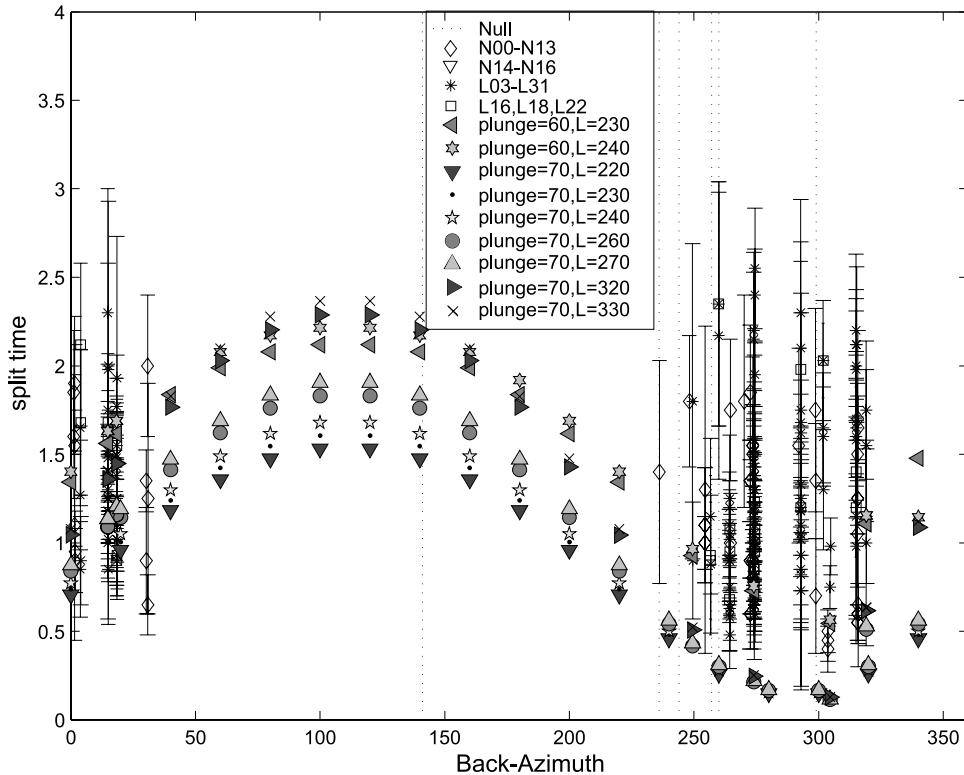


Figure 5b.

found evidence for a plunging axis of symmetry in anisotropy north of the Mendocino triple junction. They suggest that the subduction of the Juan de Fuca plate has caused the plunging anisotropy.

The codes used to perform this modeling were acquired from Renate Hartog [Hartog and Schwartz, 2000]. They perform a grid search over a suite of symmetry axis azimuths, plunges, and path lengths for 4% anisotropy for a single anisotropic layer, comparing splitting parameters predicted from each model with those observed. Models with either hexagonal or orthorhombic symmetry can be explored. With hexagonal symmetry there are two symmetry values (a, and b/c), while orthorhombic models have three values (for the a, b, and c axes). As olivine anisotropy is mainly dependent upon the a-axis orientation [Christensen 1984], the hexagonal model is used in this study. The code also allows for input of specific olivine or petrological information if it is available. Though at present, no such data is available in the CD-ROM study region. An end-member model, as used in Hartog and Schwartz [2000], where olivine is perfectly aligned, is used. The percent weight of the olivine is 25%, with 75% being an isotropic medium. This composition produces elastic properties similar to those of the upper mantle values from

IASPEI91 model ($V_p = 8$ km/s, $V_s = 4.47$, $\rho = 3.32$ gm/cc), resulting in a percent anisotropy of 4% [Hartog and Schwartz, 2000]. As the choice of 4% anisotropy is due to lack of physical data, the acceptable path lengths would be larger.

The grid search over shear wave splitting measurements from stations Northern CD-ROM stations N00 to N13 (using only “good” or better measurements) results in an inclined axis model of azimuth 280° , plunge 65° (from horizontal) and a path length of 220 km or 1.5 seconds (Figure 4 and 5). The path length is converted to δt by the following equation [Hartog and Schwartz, 2000]

$$\delta t = L (V_f - V_s) / (V_f * V_s) \quad (2)$$

Where L is path length, V_f is fast S-wave velocity, and V_s is slow S-wave velocity. As can be seen by the plot of error estimates ($X^2_{\delta t}$ and X^2_{ϕ}) in Figure 4a, the model is more dependent on azimuth than on the plunge angle. This is due to the model is more dependant on azimuth than plunge. The azimuth is mainly controlled by the fast direction of shear wave splitting and the plunge is dependent on the delay times. The shear wave splitting data shows more variation in fast directions than in delay times, so such a dependency is expected. For a

given azimuth, a large range of plunge angles fit the data with similar misfit, thus the plunge angle is not well resolved. The path length also has a range of acceptable values. The model does show significant sensitivity to plunge azimuth, which is thus better resolved than the actual plunge inclination.

The misfit values were calculated by summing the squared differences of the observed and predicted values and dividing by the squared measured errors [Hartog and Schwartz, 2000]:

$$X_{\phi}^2 = \left(\sum (\phi_{\text{pred}} - \phi_{\text{obs}})^2 \right) / (\sigma_{\phi})^2, \text{ and} \\ X_{\delta t}^2 = \left(\sum (\delta t_{\text{pred}} - \delta t_{\text{obs}})^2 \right) / (\sigma_{\delta t})^2, \quad (3)$$

where ϕ_{pred} and δt_{pred} are the predicted model values, the ϕ_{obs} and δt_{obs} are the observed values and $\sigma_{\delta t}$ are the measured misfits. The smaller the chi-squared value, the better the model fits the data. Both the ϕ and δt observed values are given equal weighting in the model.

The Laramie Array data were split into three groupings based upon similarity of splitting measurements and geographic proximity to invert for models. For Laramie array southern stations L03 to L12, the resulting best fitting model has azimuth=290° (ie. plunges to the west northwest), plunge=65°, L=220 km, and δt =1.5s. Stations L13 to L22 (without L16, L18, L22) produced a best fitting model with azimuth=290°, plunge=70°, L=340 km and δt =2.3. Stations L23 to L31 resulted in a model of azimuth=270°, plunge=70°, L=270 km and δt =1.3s. Stations L16, L18 and L22 produced anomalous results when they were included with the other Laramie Array stations. Eliminating these stations from the modeling produced acceptable results. These stations have similar results to the near-by stations (Table 6; see CDROM in back cover sleeve, Figure 2, Figure 4), so the anomalous model results are difficult to explain.

Models were determined for four subsets of the data, and produced similar results. Azimuths vary between 270° and 290°, plunges from 60 to 80 and the δt 's from 1.3 to 2.3 seconds. It might be expected that there would be a variation between north CD-ROM and Laramie arrays, given that they are separated by 110 km east-west, as well as within the individual arrays, but it is striking that they still come up with similar models.

Comparing a suite of plunging symmetry axis models with a range of plunge azimuths from 270° to 300°, plunges between 50° and 70° and varying path lengths, the models in the 290°-azimuth suite best fit the observed data (shown in Figure 5). Models with plunge azimuths from 270° to 280° have lower predicted phi values in the 264° to 274° backazimuthal range than is observed. The amplitude of predicted ϕ variations is smaller in amplitude than the observed ϕ variations, except

between back-azimuth 0° to 32° and 280° to 320°. Models with plunge azimuths of 300° over estimate values of ϕ between back-azimuths 0° to 30°.

Azimuth-290° models (plunge = 60° to 70°) closely approximate the majority of the observed splitting parameter amplitude variations (Figure 5). The plunge=70°, δt -model does not fit as well as the plunge = 60° in the west and northwest back-azimuths, while the plunge=70°, ϕ -model fits better than the plunge = 60° in amplitude of variations. Choosing a path length (L) is complicated by there not being a distinct variation in split time, δt , with ϕ . The δt observed values also do not vary greatly with back-azimuth, further complicating the choice. Therefore the best fitting model has azimuth 290° +/- 10°, plunge =65° +/- 5° and δt = 1.9 +/- 0.5 seconds.

The observed null directions cluster around back-azimuth 250°, with outliers at 299° and 141° (shown as dotted lines in Figure 5). If there were a plunging symmetry axis, one would expect the nulls and small split values to be in the azimuth of plunge, as there would be no splitting observed along the axis of symmetry (if the plunge angle were the same as the incidence angle). With a plunge of 65°, incidence angles of around 25° would show nulls along back-azimuth 290°, as this would be the axis of plunging anisotropy. S-waves would have an incidence angle this large. One S-wave event recorded on the CD-ROM array, with back-azimuth 303.7 and incidence angle of about 17°, had results for two CD-ROM stations with very small δt values (Table 3 and 5; see CDROM in back cover sleeve).

Laramie southernmost stations L01 and L02 were modeled using all splitting results (good, ok and weak) and the resulting plunging symmetry axis model has symmetry axis azimuth=340°, plunge=70°, L=150 km and δt =0.9. The L01 and L02 plunge azimuth is more north-directed than the plunge axis found with the northern Laramie array stations, and points towards the other models (L01 and L02) plunging axis. These 2 stations may be influenced by the back azimuthal variations to the north as well as from different anisotropy variations to the south. As the Laramie Array did not continue further south it is difficult to discern whether this is a separate anisotropy zone, or a freznel zone complication. A similarity happens in the CD-ROM line with N14, N15 and N16.

Travel time tomography using data from the CD-ROM north array shows a high P-wave velocity anomaly dipping steeply (approximately 50 degree plunge) north [Dueker et al, 2001]. This may be indicative of a down welling piece of lithosphere that has caused a thermal anomaly or of a fossil slab with a fast velocity anomaly in the down-dip direction.

A possibility for the change between L01 and L02 to the rest of the array (with respect to ϕ and backazimuth), is that it may indicate the location of the Cheyenne Belt (Figure 2). As the Laramie array is only 50 km long, it may be difficult to locate the Cheyenne Belt through shear-wave splitting.

While SKS phases have a steep incidence angle (5° to 12°), many ray paths could go through areas north and south of the Cheyenne Belt, therefore complicating the splitting parameters. As most of the splitting events have come from the northwest and western back-azimuths, few rays sample the mantle south of the Cheyenne Belt. This may be the reason for not seeing a change in splitting parameters between L24-L25, which is north of the surface expression of the Cheyenne Belt, and L23 to the south.

Discussion

A single layer of anisotropy is an appropriate model for the southern CD-ROM stations as well as for the region between N17 to N26. North of the Cheyenne Belt a single layer is not viable, as the average fast axis for the observed data is 110° and does not intersect any data.

Neither the two layer anisotropic models nor the plunging anisotropic symmetry axis model explain all of the shear wave splitting observations perfectly. Introduction of additional free parameters, such as more than two anisotropic layers or more than one plunging symmetry axis, may fit the observed data better, but such complex modeling may not be warranted without better back-azimuthal data coverage.

With the two anisotropic layer best fitting model, the upper layer has fast axis at 120° – 160° , roughly perpendicular to the Cheyenne Belt which trends ENE-WSW, while the lower layer (layer 1) is roughly parallel to the Cheyenne Belt. As the back-azimuthal variations are noticed north of the suture zone, the variations in the upper layer may be indicative of fossil strain in the lithosphere. Layer 2 may correlate to surface deformation during orogenesis. Dikes mapped north of the Cheyenne Belt could be indicative of the anisotropy in the upper layer [Duebendorfer and Houston, 1987]. Layer 1, roughly parallel to the Cheyenne Belt, could represent the accretion event, strain during wrench fault deformation, or it could be current strain due to absolute plate motion deformation.

The plunging anisotropic symmetry axis model (Figure 5) is our preferred model. Viewed back-azimuthally a mode-90 variation could still be possible with the observed ϕ , as there are some missing polarization angles and backazimuths, but there is no mode-90 pattern with the observed δt values. As the δt values only vary minimally, small at the western and north-western back-azimuths and larger at the northern and north-eastern back-azimuths, a model that reflects this very minimal variation is preferable. Two-layer models have rapidly varying δt values, but with the plunging symmetry axis models the variation is much more gentle, as we observe.

The plunging symmetry axis model is difficult to explain by surface geology. The plunging axis might be due to asthenos-

pheric flow interacting with strong lithosphere-asthenosphere boundary topography associated with the Archean-Proterozoic transition. Such a model was suggested by Bormann et al. [1996] to explain splitting measurements in Europe. Another hypothesis is that the splitting patterns could be related to the high seismic velocity feature seen in the teleseismic travel time tomography of Dueker et al. [2001]. Down-welling associated with such a feature could cause considerable strain in the surrounding area and result in alignment of the a-axis of olivine, although one might expect more of a lateral change in inclined axis values. For the number of stations and spatial size of the consistent inclined axis, the downwelling would need to be rather large and consistent over this large area. Other splitting results in the extended region show a consistent NE-SW orientation well west of the CD-ROM array at the Snake River Plain [Schutt et al. 1998], but complex and inconsistent orientations closer to the CD-ROM array from the Deep Probe and Lodore arrays [Humphreys et al., 2001]. Without additional measurements it is difficult to assess the lateral extent of such a downwelling feature.

Another possible explanation for the northwest plunging axis of symmetry would be the combination of compressional and shear motion across the Cheyenne Belt. North-south compression combined with left-lateral shear across the Cheyenne Belt could produce the NW directed plunge axis modeled. Shear determined from surface outcrops of rocks at the Cheyenne Belt is thought to consist mostly of right-lateral motion [Duebendorfer and Houston, 1987], opposite of what we are seeing at depth.

A structural possibility, and our preferred model, as proposed by Dueker et al. [2001] would involve a “fossil slab” accreted to the bottom of the lithosphere during the Proterozoic accretion event (Figure 6). This slab could be composed of either eclogite or some anisotropically fast structure, as would be suggested by the shear wave splitting results. A fossil slab would show consistent results over a large lateral area. The tomographic results show a fast velocity feature plunging 50° to the north. Without depth constraints on the shear-wave splitting it is difficult to discern between a dipping slab with slab-parallel anisotropy and a slab with plunging anisotropy.

Conclusions

Shear wave splitting results from South CD-ROM show consistent northeast directed shear-wave splitting, indicative of either absolute plate motion (APM) and/or fossil accretion. North CD-ROM back-azimuthal results compare well with the Laramie Array splitting parameters, suggesting a common anisotropic fabric rather than laterally heterogeneous anisotropy. The azimuthal variations of splitting from both north CD-ROM

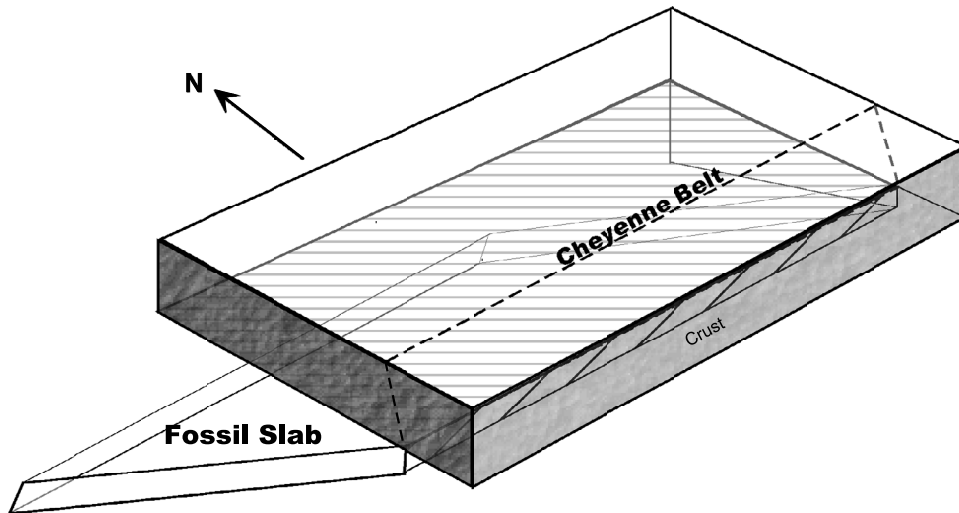


Figure 6. Block model of shear-wave splitting interpretation, showing the plunging symmetry axis as a north-dipping slab. The plunging anisotropy is only seen north of the Cheyenne Belt in the CD-ROM north data. The Laramie array tomography shows a high velocity feature that plunges to the north (Huan and Dueker, this issue). The slab may or may not touch the base of the crust, as tomography shows it at about 200km depth.

and Laramie are best modeled with a plunging axis of anisotropy. Our preferred model has azimuth $290^\circ \pm 10^\circ$, plunge $=65^\circ +5^\circ / -25^\circ$ (see Figure 4b) and $\delta t = 1.9 \pm 0.5$. As there is little depth constraint on SKS shear-wave splitting measurements, it is difficult to choose between a structural feature flush with the bottom of the crust or one that plunges. From fresnel zone arguments, the depth to the anisotropic feature, should be within the lithosphere, below the Cheyenne Belt. A lower range for anisotropy would be between 80 and 140km depth, with the majority of the anisotropy occurring above this value.

Tomography [Huan and Dueker, this issue] has shown that the best model is the one with a slab beneath the crust that plunges at high angle to the base of the crust (Figure 6). The tomography has been forward modeled as an anisotropic slab that steeply dips to the north [Huan and Dueker, this issue]. As the variations start north of the Cheyenne Belt on the CD-ROM north line, this could be the slab from a paleo-accretion event [Karlstrom et al., 2002].

Acknowledgments. We thank Renate Hartog for sharing her computer programs for modeling anisotropy with a plunging axis of symmetry, and Martha Savage for advice and discussion. Ken Dueker generously shared the Laramie array data and provided useful comments on the paper. Some figures in this paper were made with GMT [Wessel and Smith, 1998]. IRIS Passcal seismic instruments were used in this project and the Passcal Instrument Center provided assistance. This work was funded by NSF grants EAR-9614410 and EAR-0003747.

REFERENCES

- Alsina, D., and Snieder, R., Small-scale sublithospheric continental mantle deformation: constraints from SKS splitting observations, *Geophysical Journal International*, 123, 431–448, 1995.
- Bormann, P., Grunthal, G., Kind, R., and Montag, H., Upper mantle anisotropy beneath Central Europe from SKS wave splitting: effects of absolute plate motion and lithosphere-asthenosphere boundary topography?, *Journal of Geodynamics*, 22;1–2, 11–32, 1996.
- Christensen, N.I., The magnitude, symmetry and origin of upper mantle anisotropy based on fabric analysis of ultramafic tectonites, *Geophys. J.R. Astron. Soc.*, 76, 89–111, 1984.
- Crampin, S., The fracture criticality of crustal rocks, *Geophysical Journal International*, 118, 428–438, 1994.
- DeMets, C., Gordon, R.G., Argus, D.F., and Stein, S., Current plate motions, *Geophysical Journal International*, 101, 425–478, 1990.
- Duebendorfer, E.M., Houston, R.S., Proterozoic accretionary tectonics at the southern margin of the Archean Wyoming craton, *GSA Bulletin*, 98, 554–568, 1987.
- Dueker, K., Zurek, B., and Yuan, H., Western U.S. mantle; old structured lithosphere over young restless asthenosphere, *GSA Today*, 2001.
- Ehrlich, T.K. and Erlsev, E.A., The influence of the Cheyenne Belt on Cenozoic deformation in northern Colorado and southern Wyoming, *Geological Society of America*, 31; 7, 130, 1999.
- Evans, J.R., Foulger, G.R., Julian, B.R., and Miller, A.D., Crustal shear-wave splitting from local earthquakes in the Hengill triple junction, southwest Iceland, *Geophysical Research Letters*, 23, No 5, 455–458, 1996.
- Hartog, R. and Schwartz, S.Y., Subduction-induced strain in the upper mantle east of the Mendocino triple junction, California,

- Journal of Geophysical Research*, 105, No B4, 7909–7930, 2000.
- Huan Y. and Dueker, K., Upper mantle tomographic Vp and Vs images of the Middle Rocky Mountains in Wyoming, Colorado and New Mexico: Evidence for a thick heterogeneous chemical lithosphere, AGU monograph on Evolution of Rocky Mountain Lithosphere, this issue, 2002.
- Ismail, W.D., and Mainprice, D., An olivine fabric database: an overview of upper mantle fabrics and seismic anisotropy, *Tectonophysics*, 296, 145–157, 1998.
- Johnson, R.A., Karlstrom, K.E., Smithson, S.B., and Houston, R.S., Gravity profiles across the Cheyenne Belt, a Precambrian crustal suture in Southeastern Wyoming, *Journal of Geodynamics*, 445–472, 1984.
- Karlstrom, K.E. and Humphreys, E.D., Persistent influence of Proterozoic accretionary boundaries in the tectonic evolution of southwestern North America: Interaction of cratonic grain and mantle modification events, *Rocky Mountain Geology*, 33, no. 2, 161–179, 1998.
- Karlstrom, K. E., S. A. Bowring, K. R. Chamberlain, K. G. Dueker, T. Eshete, E. A. Erslev, G. L. Farmer, M. Heizler, E. D. Humphreys, R. A. Johnson, G. R. Keller, S. A. Kelley, A. Levander, M. B. Magnani, J. P. Matzel, A. M. McCoy, K. C. Miller, E. A. Morozova, F. J. Pazzaglia, C. Prodehl, H. M. Rumpel, C. A. Shaw, A. F. Sheehan, E. Shoshitaishvili, S. B. Smithson, C. M. Sneson, L. M. Stevens, A. R. Tyson, and M. L. Williams, Structure and evolution of the lithosphere beneath the Rocky Mountains: Initial results from the CD-ROM experiment, *GSA Today*, 12, no. 3, p. 4–10, 2002.
- Kay, I., Sol, S., Kendall, J.-M., Thompson, C., White, D., Asude, I., Roberts, B., and Francis, D., Shear wave splitting observations in the Archean craton of Western Superior, *Geophysical Research Letters*, 26, No 17, 2669–2672, 1999.
- Keller, G.R., Snelson, C.M., Sheehan, A.F., Dueker, K.G., Geophysical studies of crustal structure in the Rocky Mountain region: A review, *Rocky Mountain Geology*, 33, no. 2, 217–228, 1998.
- Kou, B-Y, Chen, C-C., and Shin, T-C, Split S waveforms observed in northern Taiwan: Implications for crustal anisotropy, *Geophysical Research Letters*, 21, No 14, 1491–1494, 1994.
- Leary, P.C., Crampin, S., and McEvelly, T.V., Seismic fracture anisotropy in the Earth's crust: An overview, *Journal of Geophysical Research*, 95, No B7, p 11,105–11,114, 1990.
- Levin, V., Park, J., Crustal anisotropy in the Ural Mountains fore-deep from teleseismic receiver functions. *Geophysical Research Letters*, 24, No 11, 1283–1286, 1997.
- Nicolas A. and Christensen N.I., Formation of anisotropy in upper mantle peridotites-A review, *American Geophysical Union*, 111–123, 1987.
- Ozalaybey, S. and Savage, M.K., Double-layer anisotropy resolved from S phases, *Geophysical Journal International*, 117, 653–664, 1994.
- Russo, R.M., Silver, P.G., Franke, M. Ambeh, W.B., and James, D.E., Shear-wave splitting in northeast Venezuela, Trinidad and the eastern Caribbean, *Physics of the Earth and Planetary Interiors*, 95, 251–275, 1996.
- Sandvol, E., Ni, J., Ozalaybey, S., and Shule, J., Shear-Wave splitting in the Rio Grande Rift, *Geophysical Research Letters*, 19, 2337–2340, 1992.
- Savage, M.K., Sheehan, A.F., and Lerner-Lam, A., Shear wave splitting across the Rocky Mountain Front, *Geophysical Research Letters*, 23, No B17, 2267–2270, 1996.
- Savage, M.K., Seismic anisotropy and mantle deformation: What have we learned from shear wave splitting? *Reviews of Geophysics*, 37, 65–106, 1999.
- Savage, M.K. and Sheehan, A.F., Seismic anisotropy and mantle flow from the Great Basin to the Great Plains, western United States, *Journal of Geophysical Research*, 105, No B6, 13,715–13,734, 2000.
- Schutt, D., Humphreys, E.D., and Dueker, K., Anisotropy of the Yellowstone hot spot wake, eastern Snake River Plain, Idaho, *Pure and Applied Geophysics*, 151, 443–462, 1998.
- Schutt, D. and Humphreys, E.D., Evidence for a deep asthenosphere beneath North America from western United States SKS splits, *Geology*, 29, No 4, 291–294, 2001.
- Silver, P.G., Seismic anisotropy beneath the continents: probing the depths of geology, *Annual Review Earth and Planetary Science*, 24, 385–432, 1996.
- Silver, P.G. and Chan, W.W., Shear Wave Splitting and Subcontinental Mantle Deformation, *Journal of Geophysical Research*, 96, No B10, 16,429–16,454, 1991.
- Silver, P.G. and Chan W.W., Implications for continental structure and evolution from seismic anisotropy, *Nature*, 335, 34–39, 1988.
- Tanimoto, T. and Anderson, D.L., Mapping convection in the mantle, *Geophysical Research Letters*, 11, No. 4, 287–290, 1984.
- Wessel, P. and W. H. F. Smith, New, improved version of the Generic Mapping Tools released, *EOS Trans. AGU*, 79, p. 579, 1998.
- Vinnik, L.P., Makeyeva, L.I., Milev, A., and Usenko, A.Yu., Global patterns of azimuthal anisotropy and deformations in the continental mantle, *Geophysical Journal International*, 111, 433–447, 1992.

Otina C. Fox, Geophysical Institute, PO Box 757320, Fairbanks, Alaska 99775, Voice: (907) 474–5481; Fax: (907) 474–5618, otina@giseis.alaska.edu

Anne Sheehan, Campus Box 399, Department of Geological Sciences, University of Colorado at Boulder, Boulder, Colorado 80301, Voice: (303) 492–4597; Fax: (303) 492–2606, afs@terra.colorado.edu